

Confluence of resonant laser excitation and bidirectional quantum-dot nuclear-spin polarization

C. Latta^{1*}, A. Högele^{1*†}, Y. Zhao^{2†}, A. N. Vamivakas², P. Maletinsky¹, M. Kroner¹, J. Dreiser¹, I. Carusotto³, A. Badolato⁴, D. Schuh⁵, W. Wegscheider^{5†}, M. Atature² and A. Imamoglu^{1‡}

Resonant laser scattering along with photon correlation measurements established the atom-like character of quantum dots. Here, we show that for a wide range of experimental parameters it is impossible to isolate elementary quantum-dot excitations from a strong influence of nuclear spins; the absorption lineshapes at magnetic fields exceeding 1 T indicate that the nuclear spins get polarized by an amount that ensures locking of the quantum-dot resonance to the incident laser frequency. In stark contrast to earlier experiments, this nuclear-spin polarization is bidirectional, allowing the combined electron-nuclear-spin system to track the changes in laser frequency dynamically on both sides of the resonance. This unexpected feature stems from a competition between two spin-pumping processes that attempt to polarize nuclear spins in opposite directions. We find that the confluence of laser excitation and nuclear-spin polarization suppresses the fluctuations in resonant absorption. A master-equation analysis suggests narrowing of the nuclear-spin distribution, pointing to applications in quantum information processing.

A number of ground-breaking experiments have demonstrated fundamental atom-like properties of quantum dots, such as photon antibunching¹ and radiative-lifetime-limited Lorentzian absorption lineshape² of optical transitions. Successive experiments using transport³ as well as optical spectroscopy⁴ however, revealed that the nature of hyperfine interactions in quantum dots is qualitatively different from that of atoms: coupling of a single electron spin to the mesoscopic ensemble of $\sim 10^5$ quantum-dot nuclear spins results in non-Markovian electron-spin decoherence⁵ and presents a major drawback for applications in quantum-information science. Nevertheless, it is still customary to refer to quantum dots as artificial atoms; that is, two-level emitters with an unconventional dephasing mechanism. Here, we present resonant absorption experiments demonstrating that for a wide range of system parameters, such as the gate voltage, the length of the tunnel barrier that separates the quantum dots from the back contact and the external magnetic field, nuclear spins strongly modify the signatures of elementary optical excitations. We determine that the striking locking effect of any quantum-dot transition to an incident near-resonant laser, which we refer to as dragging, is associated with dynamic nuclear-spin polarization; in stark contrast to previous experiments^{6–12}, the relevant nuclear-spin polarization is bidirectional and its orientation is determined simply by the sign of the excitation laser detuning. We find that fluctuations in the quantum-dot transition energy, either naturally occurring² or introduced by externally modulating the Stark field, are suppressed when the laser and the quantum-dot resonances are locked. We also find that when the exchange interaction between the confined quantum-dot electron and the nearby electron Fermi sea that leads to incoherent spin-flip co-tunnelling¹³ is sufficiently strong,

it can suppress the confluence of laser and quantum-dot transition energies by inducing fast nuclear-spin depolarization¹⁴.

Locking of quantum-dot resonances to an incident laser

For a single-electron-charged quantum dot, the elementary optical excitations lead to the formation of trion states (X^-) that are tagged by the angular momentum projection (pseudo-spin) of the optically generated heavy hole (Fig. 1a). In the absence of an external magnetic field ($B_{\text{ext}} = 0$ T), the absorption lineshapes associated with these optical excitations are Lorentzian (Fig. 1b), with a linewidth $\Delta\nu \sim 2.0\Gamma$; here, $\Gamma \sim 1 \mu\text{eV}$ is the spontaneous emission rate of the trion state. For $B_{\text{ext}} > 100$ mT, the coherent coupling between the (ground) electronic spin states induced by the transverse component of the (quasi-static) nuclear Overhauser field is suppressed¹⁵: in this limit, the optical excitations of the quantum dot can be considered as forming two weakly coupled two-level systems (Fig. 1a), where the blue- (red-) trion transition is associated with a quantum-dot electron initially in state $|\uparrow_z\rangle$ ($|\downarrow_z\rangle$). Figure 1c shows absorption measurements carried out at $B_{\text{ext}} = 4.5$ T when the laser field with frequency ω_L is tuned across the blue-trion resonance (transition energy $\hbar\omega_X$). For a laser that is tuned from an initial blue detuning to a final red detuning with respect to the quantum-dot resonance (red line in Fig. 1c), we find that the absorption is abruptly turned on when we reach $\omega_L \sim \omega_X + 2\Delta\nu$; the absorption strength then remains essentially fixed at its maximal value until we reach $\omega_L \sim \omega_X - 7\Delta\nu$, where it abruptly goes to zero. A laser scan in the opposite direction (blue line) shows a complementary picture with the trion absorption strength remaining close to its peak value for laser frequencies that are blue detuned from the bare trion resonance by as much as $7\Delta\nu$.

¹Institute of Quantum Electronics, ETH-Zurich, CH-8093, Zurich, Switzerland, ²Cavendish Laboratory, University of Cambridge, JJ Thomson Ave, Cambridge CB3 0HE, UK, ³CNR-INFM BEC Center and Dipartimento di Fisica, Università di Trento, via Sommarive 14, I-38050 Povo, Trento, Italy,

⁴Department of Physics and Astronomy, University of Rochester, Rochester, New York 14627, USA, ⁵Institut für Experimentelle und Angewandte Physik, Universität Regensburg, Regensburg, Germany. *These authors contributed equally to this work. †Present address: Ludwig-Maximilians-Universität München, Fakultät für Physik und CeNS, Geschwister-Scholl-Platz 1, 80539 München, Germany (A.H.). Physikalisches Institut, Ruprecht-Karls-Universität Heidelberg, Philosophenweg 12, Heidelberg 69120, Germany (Y.Z.); Solid State Physics Laboratory, ETH Zurich, 8093 Zurich, Switzerland (W.W.).

‡e-mail: imamoglu@phys.ethz.ch.

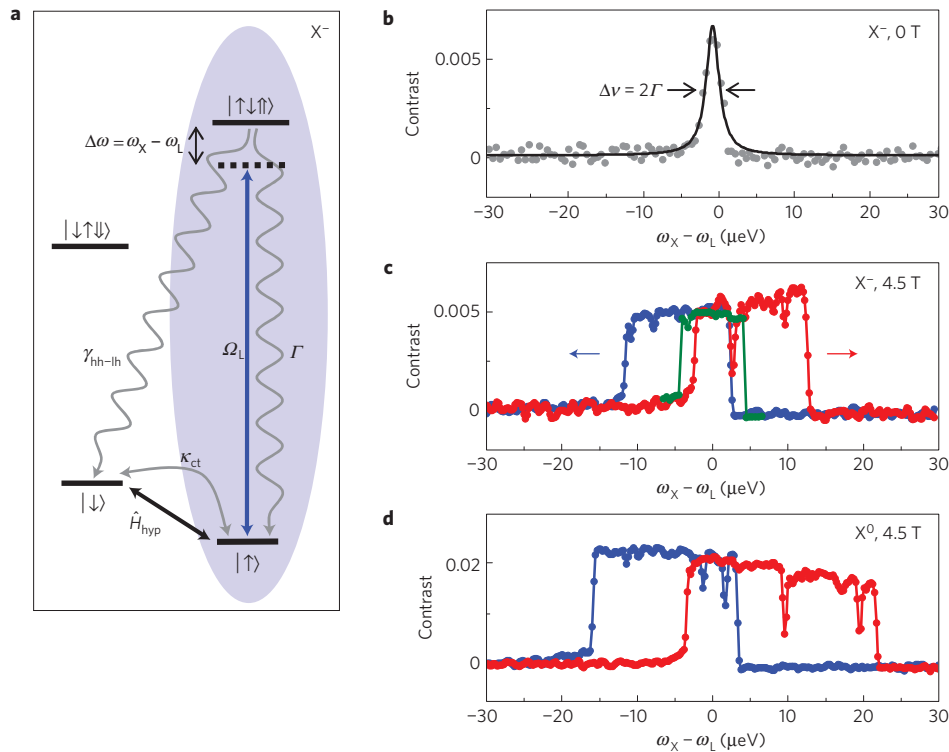


Figure 1 | Dragging of quantum-dot resonances. **a**, An energy-level diagram of a single-electron-charged quantum dot: an external magnetic field enables spin-selective excitation of Zeeman-split trion (X^-) states. A right-hand circularly polarized laser with Rabi frequency Ω_L (blue arrow) and detuning $\Delta\omega = \omega_X - \omega_L$ couples the higher-energy Zeeman branch between the spin-up electron ground state $|\uparrow\rangle$ and the trion state $|\uparrow\downarrow\uparrow\rangle$. The relevant decoherence processes (radiative decay Γ , co-tunnelling κ_{ct} and heavy-hole/light-hole mixing γ_{hh-lh}) are indicated by grey arrows. **b,c**, Trion absorption spectra at zero magnetic field (Lorentzian fit with a linewidth of 2 μeV) (**b**) and at 4.5 T (**c**). For magnetic fields exceeding 1 T, the on-resonance scattering is maintained over many natural linewidths to both sides of the bare resonance. The red (blue) spectra show data obtained by tuning the laser from an initial blue (red) to a final red (blue) detuning from the quantum-dot resonance. The green trace shows the energy range over which resonant absorption is recovered in fixed-laser-detuning experiments (see Fig. 3c). **d**, The dragging effect is even more prominent in the absorption spectra of the blue Zeeman branch of the neutral exciton X^0 at 4.5 T. In all experiments, the temperature was 4.2 K.

The absorption scans of Fig. 1c show that the trion resonance locks on to the laser frequency and can be dragged to either higher or lower energies by tuning the laser frequency, provided that the scan frequency-step size is small (see Supplementary Information). We observe this dragging effect for a wide range of laser Rabi frequencies Ω_L ranging from $\sim 0.3\Gamma$ to 3Γ . We also emphasize that dragging is not a simple line-broadening effect: the area of the absorption curve is an order of magnitude larger than its $B_{\text{ext}} = 0$ T counterpart.

It is well known that the optical response of a neutral quantum dot for $B_{\text{ext}} < 1$ T is qualitatively different, owing to the role of electron-hole exchange interaction¹⁶. To assess the generality of the dragging phenomenon, we investigated the response of a neutral quantum dot for $B_{\text{ext}} \geq 2$ T: despite an energy level diagram that is substantially different from that of a single-electron-charged quantum dot, the bright exciton transitions of a neutral quantum dot exhibit absorption lineshapes (Fig. 1d) that are qualitatively similar to that of a trion. In fact, we observe that typical dragging widths for neutral quantum-dot exciton transitions are significantly larger than that of trion transitions.

Further insight into the locking phenomenon shown in Fig. 1c,d can be gained by studying its dependence on basic system parameters. Figure 2 shows the two-dimensional map of resonant absorption as a function of laser frequency and gate voltage V_g for two different sample structures exhibiting radically different ranges of the co-tunnelling rate. Figure 2a shows the two-dimensional absorption map of a quantum dot that is separated from the Fermi sea by a 25 nm GaAs barrier (sample A): each horizontal cut is obtained by scanning the gate voltage for a fixed laser frequency.

The red (blue) bars show data obtained by scanning the gate voltage such that the detuning $\Delta\omega = \omega_X - \omega_L$ decreases (increases). We estimate the co-tunnelling rate κ_{ct} for this sample at the centre of the absorption plateau ($V_g = 200$ mV) to be $1 \times 10^6 \text{ s}^{-1}$ from electron-spin pumping experiments carried out at $B_{\text{ext}} = 0.3$ T (ref. 17). We observe that the bidirectional dragging effect is strongest in the plateau centre and is completely suppressed at the edges ($V_g \sim 160$ mV and $V_g \sim 260$ mV).

Figure 2b shows absorption maps for a quantum dot that is separated from the Fermi sea by a 43 nm tunnel barrier (sample B) at two different values of B_{ext} (2 and 6 T): each vertical cut is obtained by scanning the laser energy for a fixed gate voltage. The data presented in Fig. 2b are obtained for a narrow range of V_g near the edge of the charging plateau: the large tunnel barrier drastically suppresses the tunnel coupling, such that the highest κ_{ct} (obtained at the plateau edges) coincides with the lowest rate obtained for sample A. Consequently, bidirectional dragging in sample B extends all the way out to the edge of the charging plateau, whereas in the plateau centre absorption disappears completely owing to electron-spin pumping into the $|\downarrow_z\rangle$ state¹⁵. The overall range for dragging is $\sim 40 \mu\text{eV}$ ($\sim 20 \mu\text{eV}$) for $B_{\text{ext}} = 6$ T ($B_{\text{ext}} = 2$ T) and is symmetrically centred at the bare X^- transition energy. Experiments carried out on quantum dots in all samples showed that the dragging width increases sublinearly with B_{ext} beginning at ~ 1 T. Further experiments carried out on sample C (not shown) with quantum dots separated by a 15 nm tunnel barrier from an electron reservoir and exhibiting $\kappa_{ct} > \Gamma$ throughout the plateau, did not show dragging effects. These

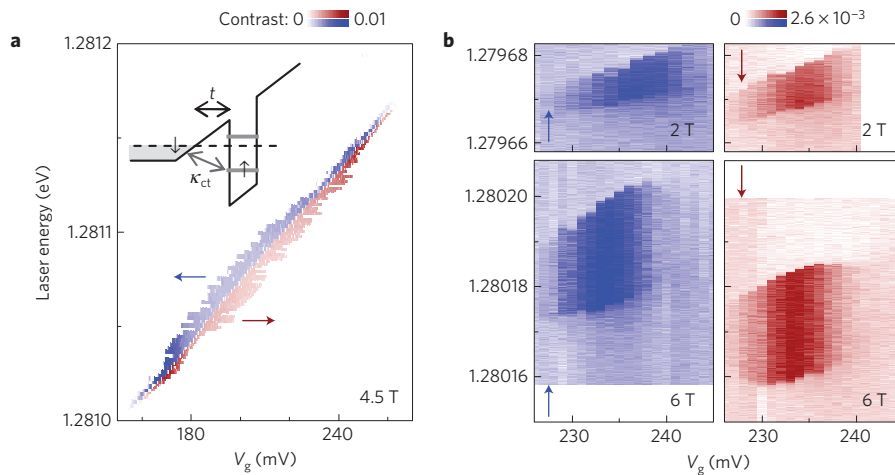


Figure 2 | Dependence of dragging on system parameters. Two-dimensional absorption maps of the blue-trion Zeeman branch as a function of gate voltage and laser energy. The red (blue) arrows indicate the scan direction with decreasing (increasing) laser detuning $\Delta\omega = \omega_X - \omega_L$. **a**, An absorption map recorded at 4.5 T for a quantum dot in sample A with a 25 nm tunnelling barrier: the data were obtained by keeping the laser energy fixed and scanning the gate voltage. The inset illustrates the exchange coupling to the Fermi reservoir that flips the quantum-dot electron spin by means of co-tunnelling events. The co-tunnelling rate is minimum in the centre and maximum at the edges of the stability plateau; the dragging width scales inversely with the co-tunnelling rate κ_{ct} . **b**, Absorption maps of a quantum dot in sample B with a 43 nm tunnelling barrier that were obtained by scanning the laser at a fixed gate voltage in external magnetic fields of 2 T and 6 T. Finite absorption contrast is restricted to the edge of the single-electron charging plateau owing to electron-spin pumping. The set of data is complementary to **a** and shows that dragging is independent of whether the laser or the gate voltage is scanned. The dragging width increases sublinearly with increasing strength of the external magnetic field.

results show that locking of the quantum-dot resonance to the incident laser energy is possible provided that the co-tunnelling rate of the quantum-dot electron satisfies $\kappa_{ct} < 10^8 \text{ s}^{-1}$. We observed that the neutral exciton transition of the sample B quantum dot shows dragging even at the centre of the plateau where we expect $\kappa_{ct} \leq 1 \text{ s}^{-1}$ (not shown). This observation suggests that dragging of the quantum-dot resonances takes place even for quantum dots that are completely isolated from a back contact. Finally, we note that bidirectional dragging is also observed when the red-trion or the red-Zeeman neutral-exciton transitions are driven by a resonant laser field; in contrast to the blue-trion (Fig. 1c) and high-energy neutral-exciton (Fig. 1d) transitions, the forward and backward scans in this case are highly asymmetric.

Bidirectional nuclear-spin polarization

The disappearance of dragging with increasing co-tunnelling rate or vanishing external magnetic field strongly suggests that locking of the quantum-dot optical transition to the laser frequency is associated with dynamic nuclear-spin polarization (DNSP). Recent studies carried out with laser fields resonant with the excited-state transitions of quantum dots have shown that the nuclear-spin depolarization rate has a strong dependence on the electron-spin co-tunnelling rate¹⁴; these experiments also demonstrated that when the quantum dot is neutral, the nuclear spins do not depolarize even on timescales exceeding an hour¹⁸. To confirm that DNSP indeed has a key role in our experimental findings, we have carried out experiments to determine the relevant timescales for the build-up and decay of the locking phenomenon.

Figure 3a shows a set of experiments that reveal the timescales associated with the decay of the DNSP generated during dragging, for the trion transition in sample A at $B_{\text{ext}} = 4.5 \text{ T}$ and V_g that minimizes the coupling to the Fermi sea. The procedure used in these experiments is to first drag the quantum-dot trion transition by about $5\Delta\nu$ to the red side of the bare resonance ω_X , and then to abruptly change the detuning between the trion and the laser field by a millisecond voltage ramp. The effect of this ramp is to set a new detuning condition $\omega_X - \omega_L \leq 4\Delta\nu$, which in turn results in an instantaneous loss of the absorption contrast. We

observed that after a waiting time of the order of seconds, the initially vanishing absorption strength recovered its maximum value (Fig. 3a, red-coded data). By repeating this experiment for a set of final detunings ranging from $4\Delta\nu$ to 0, we determined the characteristic exponential timescale for contrast recovery to be $\tau_d = 4.9 \pm 0.9 \text{ s}$. When we repeated the same experiment by first dragging the trion resonance to the blue side of the bare resonance and monitoring absorption for a final set of detunings satisfying $\omega_X - \omega_L \geq -4\Delta\nu$, we determined a contrast recovery time of $\tau_d = 3.7 \pm 0.7 \text{ s}$ (Fig. 3a, blue-coded data). These results provide information about the decay time of the DNSP that is built up during the dragging process; as DNSP decays in the absence of a resonant laser, the Zeeman-shifted trion resonance frequency changes until it once again reaches the resonance condition with the laser field. As the presence of a laser field that is detuned by less than $2\Delta\nu$ would speed up also the recovery of resonant absorption (see Fig. 3c), the timescales we obtain for the decay of the nuclear-spin polarization in this experiment could be regarded as an upper bound on the nuclear-spin depolarization rate. The DNSP decay times that we determine are in agreement with the values one would extrapolate from earlier experiments where $\kappa_{ct} \sim 10^8 \text{ s}^{-1}$ resulted in DNSP decay times of the order of a few milliseconds at $B_{\text{ext}} = 0.2 \text{ T}$ (ref. 14). When we repeated the experiment of Fig. 3 for the neutral quantum-dot exciton transition, we observed that the absorption contrast for $|\omega_X - \omega_L| < 4\Delta\nu$ always remained zero, indicating that the DNSP decay time was much longer than our measurement time of $\sim 1 \text{ h}$; this observation is in perfect agreement with earlier experiments¹⁸. Finally, we remark that the bistable behaviour of resonant absorption contrast that is evident in vertical line cuts taken from the data in Fig. 3a (shown in Fig. 3b) is very characteristic of nonlinear nuclear-spin dynamics in quantum dots^{10,11}.

Figures 1 and 2 demonstrate that the response of a quantum dot to a given laser detuning strongly depends on how the system reaches that particular detuning. To determine the quantum-dot optical response in the absence of such memory effects, we have carried out another set of experiments, where we first set the laser frequency to a large negative detuning with completely negligible excitation of the trion and kept the quantum dot in a parameter

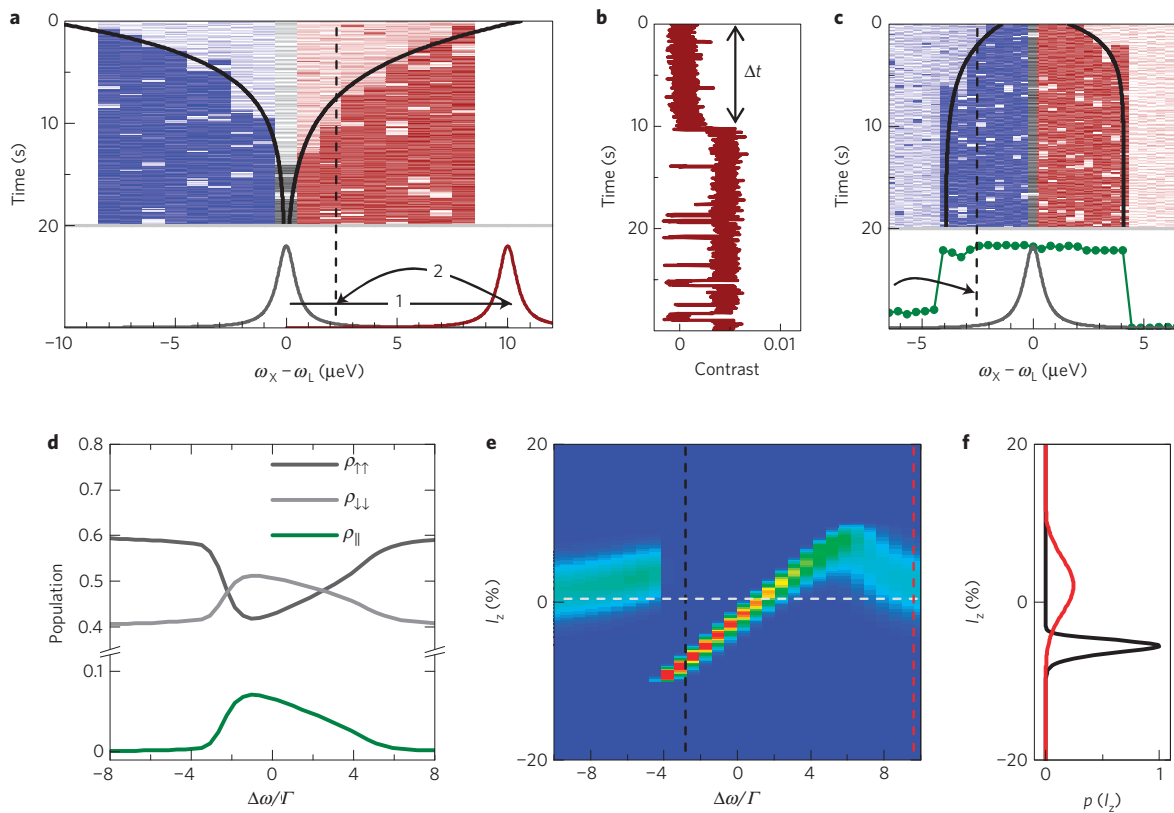


Figure 3 | Bidirectional nuclear-spin polarization. Absorption signal (light blue/red: no absorption; dark blue/red: large absorption) as a function of laser detuning and time. **a**, Decay: the nuclear spins are polarized by dragging the resonance by $10 \mu\text{eV} \simeq 5\Delta\nu$ (arrow 1). The detuning condition is instantly changed to $|\omega_X - \omega_L| \leq 8 \mu\text{eV}$ (arrow 2). The recovery of the absorption signal after a time Δt indicates that the nuclear-spin polarization has decayed. **b**, Time trace of the resonance signal along the dashed line in **a**. **c**, Build-up: after completely depolarizing nuclear spins, the laser is set to a finite detuning (arrow). The recovery of the absorption indicates a build-up of nuclear-spin polarization. **d**, Simulation of the quantum-dot level population in the steady state for the experiment described in **c**. **e**, Probability distribution $p(I_z)$ for obtaining a value I_z of the Overhauser field for a detuning range $(-10\Delta\nu, 10\Delta\nu)$. The simulation shows bidirectional nuclear-spin polarization as well as a reduction in the Overhauser field variance when the system is locked on to resonance. **f**, $p(I_z)$ for two detunings marked by the dashed lines in **e**.

regime with a strong co-tunnelling rate for several seconds. This procedure allows the quantum-dot nuclear spins to thermalize with the lattice, which in turn ensures vanishing nuclear-spin polarization. We then abruptly changed the voltage on a milliseconds timescale, thereby instantaneously establishing $|\omega_X - \omega_L| \leq 7\Delta\nu$. Subsequently, we observed the time dependence of the absorption signal at this fixed detuning. Figure 3c shows that for a detuning range of $3\Delta\nu \geq |\omega_X - \omega_L| > \Delta\nu$, the absorption strength grows from zero to its maximum value on a timescale of a few seconds, whereas within $|\omega_X - \omega_L| \leq \Delta\nu$ the on-resonance condition is established on a timescale below the temporal resolution limit of a few milliseconds in our experiment. Even though the frequency range over which the quantum dot is able to lock on to the laser field is identical for red and blue detunings, the absorption recovery time is a factor of two slower for a laser that is tuned to the blue side of the bare trion resonance. Experimentally we find $\tau_b = 3.6 \pm 0.8$ s for blue, and 2.1 ± 0.7 s for red-laser detunings (solid lines in Fig. 3c). We also note that the frequency range over which full absorption is recovered in these fixed-laser-frequency dragging experiments (green curve in Fig. 1c and Fig. 3c) is narrower than that of the dynamical dragging bandwidth obtained by tuning the laser across the resonance (red and blue curves in Fig. 1c).

Perhaps the most unexpected feature of our experiments is the remarkably symmetric dragging effect that indicates bidirectional DNSP; this observation is in stark contrast with recent experiments that demonstrated unidirectional dragging of the electron-(microwave) spin resonance and the bistability of the coupled

quantum-dot electron–nuclei system¹⁹. These results, obtained concurrently, could be understood as arising from a dominant nuclear-spin pumping process that is a nonlinear function of the degree of DNSP and competes with the nuclear-spin depolarization processes^{20,21}.

We understand the bidirectionality of DNSP by considering that the optical excitation of the quantum-dot blue-trion transition (Fig. 1a) induces two competing nuclear-spin pumping processes that try to polarize quantum-dot nuclear spins in two opposite directions and that have a different functional dependence on the effective laser detuning $\Delta\tilde{\omega} = \tilde{\omega}_X - \omega_L$; here, $\tilde{\omega}_X$ is the quantum-dot blue-trion transition energy shifted/renormalized by DNSP. The reverse-Overhauser process²⁰, associated with hyperfine-assisted spin-flip Raman scattering^{6,7}, polarizes the nuclear spins along the $+\hat{z}$ direction and depends linearly on the absorption rate $W_{\text{abs}} = \Omega_L^2 \Gamma / (4\Delta\tilde{\omega}^2 + 2\Omega_L^2 + \Gamma^2)$ from the $|\uparrow_z\rangle$ state. This process dominates for large $|\Delta\tilde{\omega}|$. In contrast, the Overhauser process that polarizes the nuclear spins along $-\hat{z}$ is effected by optical pumping of the electron spin by means of spin-flip Raman scattering induced by heavy-hole/light-hole mixing, together with a resonant-absorption-induced spin dephasing; we assume that the strength of this spin dephasing/decay rate is proportional to W_{abs} (see Supplementary Information). As the excess spin population in state $|\downarrow_z\rangle$ is also proportional to W_{abs} , the overall spin-dephasing-induced Overhauser processes depend on W_{abs}^2 and determine the direction of DNSP for small values of $|\Delta\tilde{\omega}|$. The two opposing processes balance each other out at a finite red or blue detuning²⁰.

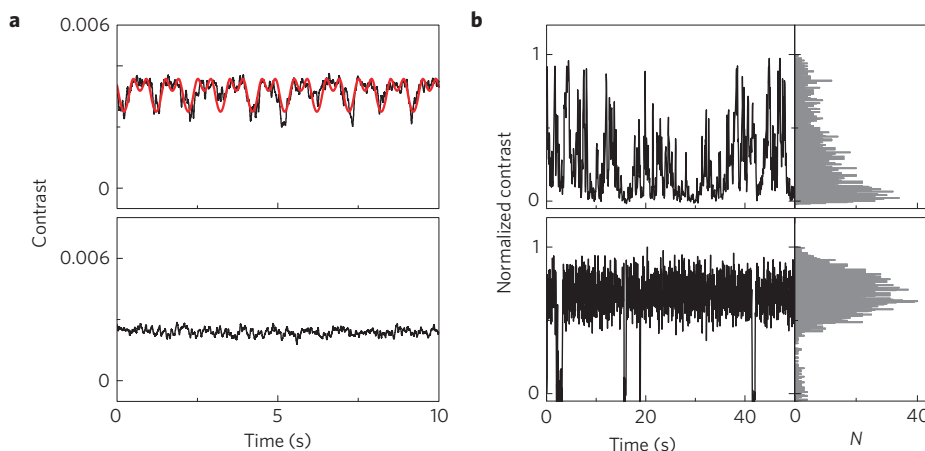


Figure 4 | Suppression of fluctuations in quantum-dot resonance frequency. **a**, Suppression of the fluctuations in the resonant absorption signal when the dragging condition is satisfied in sample B. Upper panel: the measured absorption contrast as a function of time for a fixed laser frequency at $B_{\text{ext}} = 0$ T in the presence of a 1 Hz sinusoidal gate voltage modulation. The modulation amplitude corresponds to a shift of the trion transition by $\Delta\nu/2$ around the exact resonance condition. Lower panel: the corresponding time-dependent fixed-laser-frequency absorption contrast at $B_{\text{ext}} = 4$ T when dragging is present. The signal shows full compensation of the externally induced detuning modulation. **b**, The fluctuations in the resonant absorption signal observed for the quantum dot in sample A at 0 T (upper panel) are suppressed in the presence of dragging at 4.5 T (lower panel); the data in both panels of **b** are normalized to the peak absorption contrast obtained at the corresponding magnetic field.

The red detuning ($\tilde{\omega}_X > \omega_L$) where the net polarization rate vanishes is a stable point of the coupled system (see Supplementary Fig. S4): tuning the laser closer to (away from) resonance would lead to an enhanced Overhauser (reverse-Overhauser) process, which would ensure that the trion resonance is blueshifted (redshifted) until the stable point is once again reached. In addition to the Overhauser and reverse-Overhauser channels, there are pure DNSP decay processes that are mediated either by exchange interactions between the quantum-dot electron and the Fermi sea or by electron–phonon interactions. The unexpected dragging observed on the quantum-dot X^0 transition could also be understood as arising from a similar competition between detuning-dependent Overhauser and reverse-Overhauser processes.

The interplay between the two polarization channels ensures that DNSP in either direction can be attained; the maximum DNSP that can be achieved is in turn determined by the co-tunnelling or phonon-assisted DNSP decay processes. To gain further insight into this interplay, we have solved the master equation describing the evolution of the coupled electron–nuclear-spin system in the steady state (see the Methods section and Supplementary Information).

Figure 3d shows the steady-state electron spin and trion populations evaluated for a range of fixed laser detunings using this procedure. The trion population as a function of the laser detuning is a direct measure of the absorption strength that we experimentally determined in Fig. 3c: we observe that our model reproduces the broadened absorption profile but does not capture the sharp change in the absorption strength that we observe experimentally. This discrepancy could be due to the fact that our calculations give the steady-state values, which may be practically impossible to observe experimentally. Figure 3e shows the probability distribution $p(I_z) = \sum_1 |I_z\rangle \rho |I_z\rangle$ for obtaining a specific value I_z of the Overhauser field, evaluated for the same range of parameters used in Fig. 3c: these results demonstrate that the bidirectional dragging indeed originates from a bidirectional DNSP. Perhaps more important is the fact that $p(I_z)$ reveals an impressive reduction in the Overhauser field variance by more than a factor of five, when dragging is present (Fig. 3f).

Suppression of fluctuations in transition energy

The experiments shown in Figs 1–3 as well as the numerical results shown in Fig. 3d demonstrate the existence of a feedback mechanism that polarizes the necessary number of nuclear spins

needed to shift the transition energy in a way to maintain resonance with the excitation laser. Consequently, fluctuations in the quantum-dot transition energy that would normally lead to a fluctuating absorption signal should be suppressed by such a compensation mechanism provided that the fluctuations occur within the effective feedback bandwidth. Figure 4a shows the time dependence of the absorption signal for $B_{\text{ext}} = 0$ T and $B_{\text{ext}} = 4$ T for sample B in the presence of external modulation of the trion resonance energy. The upper panel shows a time record of the on-resonance signal for $B_{\text{ext}} = 0$ T with 10 ms time resolution and in the presence of a controlled disturbance of the trion transition energy. This is achieved by introducing a 1 Hz sine modulation on the gate voltage with a peak-to-peak voltage amplitude corresponding to $\Delta\nu/2$ through the Stark shift. The $B_{\text{ext}} = 0$ T signal on resonance clearly reproduces this modulation as the transition goes in and out of resonance with the laser consistent with the expected signal drop. However, the $B_{\text{ext}} = 4$ T on-resonance signal shows complete suppression of this external disturbance of the transition energy (lower panel). The same experiment repeated for higher frequencies shows that suppression works at least up to 10 Hz, determining the relevant bandwidth for Overhauser field dynamics for this particular quantum dot and gate voltage. When the disturbance is in the form of a square-wave modulation of peak-to-peak amplitude less than $\Delta\nu$, suppression is still present, whereas beyond $\Delta\nu$ modulation, no suppression can be seen regardless of the modulation frequency. This is consistent with the slow timescale of DNSP build-up in comparison with the abrupt jump of the transition under square-wave modulation.

Even in the absence of an external perturbation, most quantum dots show time-dependent fluctuations in ω_X (ref. 2): these fluctuations could arise either from the electromagnetic environment of the quantum dot or fluctuating nuclear Overhauser field. Figure 4b (upper panel) shows a typical time record of the resonant absorption signal of the sample A quantum dot together with the corresponding distribution function for $\Omega_L \sim \Gamma$: in contrast to the sample B quantum dot studied in Fig. 4a, we observe up to 100% fluctuations in the resonant absorption signal, which is in turn a factor of three larger than our noise floor. In contrast, for $B_{\text{ext}} = 4.5$ T (Fig. 4b, lower panel), we find that the fluctuations in the absorption signal are reduced to the noise-floor. The absorption signal occasionally drops to a low value, indicating bistability in the response of the coupled electron–nuclei system

to the resonant laser field. The frequency of jumps in absorption strength depends strongly on the system parameters; in particular the sample B quantum dot practically never showed jumps during the observation period exceeding 10 s.

Having demonstrated that the locking of the quantum-dot resonance to the incident laser frequency by means of selective DNSP strongly damps out the fluctuations in the electronic transition energy, we address the possibility of suppressing the time-dependent fluctuations in the nuclear Overhauser field^{12,22}. Given that the effective Zeeman shift associated with the r.m.s. Overhauser field of the quantum-dot nuclei B_{nuc} is comparable to the spontaneous emission rate, we would expect that the fluctuations in the Overhauser field would lead to sizable fluctuations of the resonant absorption signal on timescales that are characteristic for the Overhauser field (a few seconds). As we lack controlled experiments exclusively demonstrating the role of the Overhauser field fluctuations on the absorption signal, we could claim only that the experiments shown in Fig. 4 provide indirect evidence for a suppression of nuclear Overhauser field fluctuations that is predicted by our theoretical model (Fig. 3e and f).

We emphasize that a narrowing of the Overhauser field variance would have remarkable consequences for quantum-information processing based on spins. In particular, a major limitation for experiments detecting spin coherence in quantum dots is the random, quasi-static Overhauser field that leads to an inhomogeneous broadening of the spin transition with a short T_2^* time³. Suppression of the long-timescale Overhauser field fluctuations by laser dragging may be used to ensure that the time/ensemble-averaged spin coherence measurements yield a dephasing time that is limited only by the fundamental spin decoherence processes^{23–25}. Whereas replacing the more traditional spin-echo techniques with laser dragging would represent a practical advantage for optical experiments, a more intriguing possibility would be the slowing down of nuclear-spin dynamics by a combination of large inhomogeneous quadrupolar shifts¹⁸ and dragging, which may in turn prolong the inherent electron-spin coherence time.

Methods

Theoretical model. To obtain a tractable master equation for $N \sim 1,000$ spins, we have modelled the nuclear-spin system in the Dicke basis of collective spin states $|I, I_z\rangle$ having a total angular momentum I ($0 \leq I \leq N/2$) and that couple to the quantum-dot electron by means of hyperfine interaction. States belonging to different I but having identical spin projection I_z along B_{ext} are assumed to be coupled weakly by incoherent jump processes. This coupling would have been identically zero, if the hyperfine coupling to each nuclei had been identical. The overall contribution of each I to the coupled dynamics is weighted by the number $D(I)$ of allowed permutation-group quantum numbers associated with that total angular momentum²⁶. The master equation is obtained by first applying a Schrieffer–Wolff transformation that eliminates the flip-flop terms of the hyperfine interaction, and then tracing over the electron-spin and radiation field reservoirs in the Born–Markov limit.

Experimental details. The InGaAs quantum dots studied in this work were grown by molecular beam epitaxy and are embedded in a Schottky-diode structure. An applied gate voltage allows for discrete charging of the quantum dot with single electrons. For all of the experiments, the samples were placed in a liquid-helium bath cryostat at 4.2 K. The cryostat was equipped with a 7 T superconducting magnet. The absorption experiments were carried out by focusing the beam of a power-stabilized single-mode tunable laser diode on a single quantum dot. The change in transmission through the sample was recorded by a Si photodiode. To increase the signal-to-noise ratio, a lock-in technique was used where the gate voltage was modulated.

Received 21 April 2009; accepted 3 July 2009; published online 16 August 2009

References

- Michler, P. *et al.* A quantum dot single-photon turnstile device. *Science* **290**, 2282–2285 (2000).
- Högele, A. *et al.* Voltage-controlled optics of a quantum dot. *Phys. Rev. Lett.* **93**, 217401 (2004).
- Petta, J. R. *et al.* Coherent manipulation of coupled electron spins in semiconductor quantum dots. *Science* **309**, 2180–2184 (2005).
- Braun, P. F. *et al.* Direct observation of the electron spin relaxation induced by nuclei in quantum dot. *Phys. Rev. Lett.* **94**, 116601 (2005).
- Khaetskii, A., Loss, D. & Glazman, L. Electron spin decoherence in quantum dots due to interaction with nuclei. *Phys. Rev. Lett.* **88**, 186802 (2002).
- Gammon, D. *et al.* Electron and nuclear spin interactions in the optical spectra of single GaAs quantum dots. *Phys. Rev. Lett.* **86**, 5176–5179 (2001).
- Eble, B. *et al.* Dynamic nuclear polarization of a single charge-tunable InAs/GaAs quantum dot. *Phys. Rev. B* **74**, 081306 (2006).
- Koppens, F. H. L. *et al.* Driven coherent oscillations of a single electron spin in a quantum dot. *Nature* **442**, 766–771 (2006).
- Lai, C. W., Maletinsky, P., Badolato, A. & Imamoglu, A. Knight-field-enabled nuclear spin polarization in single quantum dots. *Phys. Rev. Lett.* **96**, 167403 (2006).
- Maletinsky, P. *et al.* Nonlinear dynamics of quantum dot nuclear spins. *Phys. Rev. B* **75**, 035409 (2007).
- Tartakovskii, A. *et al.* Nuclear spin switch in semiconductor quantum dots. *Phys. Rev. Lett.* **98**, 026806 (2007).
- Reilly, D. *et al.* Suppressing spin qubit dephasing by nuclear state preparation. *Science* **321**, 817–821 (2008).
- Smith, J. M. *et al.* Voltage control of the spin dynamics of an exciton in a semiconductor quantum dot. *Phys. Rev. Lett.* **94**, 197402 (2005).
- Maletinsky, P. *et al.* Dynamics of quantum dot nuclear spin polarization controlled by a single electron. *Phys. Rev. Lett.* **99**, 056804 (2007).
- Atatüre, M. *et al.* Quantum-dot spin-state preparation with near-unity fidelity. *Science* **312**, 551–553 (2006).
- Bayer, M. *et al.* Electron and hole g factors and exchange interaction from studies of the exciton fine structure in In_{0.60}Ga_{0.40}As quantum dots. *Phys. Rev. Lett.* **82**, 1748–1751 (1999).
- Dreiser, J. *et al.* Optical investigations of quantum dot spin dynamics as a function of external electric and magnetic fields. *Phys. Rev. B* **77**, 075317 (2008).
- Maletinsky, P., Kroner, M. & Imamoglu, A. Breakdown of the nuclear spin temperature approach in quantum dot demagnetization experiments. *Nature Phys.* **5**, 407–411 (2009).
- Vink, I. T. *et al.* Locking electron spins into magnetic resonance by electron-nuclear feedback. *Nature Phys.* doi:10.1038/nphys1366 (2009).
- Rudner, M. & Levitov, L. Electrically driven reverse Overhauser pumping of nuclear spins in quantum dots. *Phys. Rev. Lett.* **99**, 246602 (2007).
- Danon, J. & Nazarov, Y. V. Nuclear tuning and detuning of the electron spin resonance in a quantum dot: Theoretical consideration. *Phys. Rev. Lett.* **100**, 056603 (2008).
- Greilich, A. *et al.* Mode locking of electron spin coherences in singly charged quantum dots. *Science* **313**, 341–345 (2006).
- Coish, W. A. & Loss, D. Hyperfine interaction in a quantum dot: Non-Markovian electron spin dynamics. *Phys. Rev. B* **70**, 195340 (2004).
- Taylor, J. M. *et al.* Relaxation, dephasing, and quantum control of electron spins in double quantum dots. *Phys. Rev. B* **76**, 035315 (2007).
- Cywinski, L., Witzel, W. M. & Das Sarma, S. Electron spin dephasing due to hyperfine interactions with a nuclear spin bath. *Phys. Rev. Lett.* **102**, 057601 (2009).
- Taylor, J. M., Imamoglu, A. & Lukin, M. D. Controlling a mesoscopic spin environment by quantum bit manipulation. *Phys. Rev. Lett.* **91**, 246802 (2003).

Acknowledgements

We thank S. Fält for growing samples B and C. We also acknowledge many useful discussions with H. Türeci, J. Taylor, G. Giedke, M. Rudner and L. Levitov. This work was supported by NCCR Quantum Photonics (NCCR QP), research instruments of the Swiss National Science Foundation (SNSF), and by an ERC Advanced Investigator Grant (A.I.). The work carried out in Cambridge was supported by QIP IRC and EPSRC grant No EP/G000883/1. D.S. and W.W. would like to thank the Deutsche Forschungsgemeinschaft (DFG) and the Bundesministerium fuer Bildung und Forschung (BMBF) for financial support.

Author contributions

C.L. and A.H. carried out the experiments on samples A and C. Y.Z. and A.N.V. carried out the experiments on sample B. A.B., D.S. and W.W. grew the samples. A.I., along with C.L. and A.H., developed the model that explained the experimental observations. C.L., I.C. and A.I. did the theoretical analysis. P.M., M.K., J.D. and M.A. carried out earlier experiments and actively participated in discussions. A.H., M.A. and A.I. planned the experiments.

Additional information

Supplementary information accompanies this paper on www.nature.com/naturephysics. Reprints and permissions information is available online at <http://npg.nature.com/reprintsandpermissions>. Correspondence and requests for materials should be addressed to A.I.